Arch Virol (2010) 155:187–195
DOI 10.1007/s00705-009-0560-0

ORIGINAL ARTICLE

Acute respiratory distress syndrome induced by H9N2 virus in mice

Guangcun Deng · Jianmin Bi · Fuli Kong · Xuezhu Li · Qiang Xu · Jun Dong · Miaojie Zhang · Lihong Zhao · Zhihua Luan · Nana Lv · Jian Qiao

Received: 17 August 2009 / Accepted: 29 October 2009 / Published online: 28 November 2009

Abstract H9N2 avian influenza viruses have repeatedly caused infections in swine and humans in some countries. The purpose of the present study was to evaluate the pulmonary pathology caused by H9N2 viral infection in mice. Six- to eight-week-old BALB/c mice were infected intranasally with 1×10^4 MID_{50} of A/Chicken/Hebei/4/2008(H9N2) virus. Clinical signs, pathological changes and viral replication in lungs, arterial blood gas, and cytokines in bronchoalveolar lavage fluid (BALF) were observed at different time points after infection. A control group was infected intranasally with noninfectious allantoic fluid. H9N2-infected mice exhibited severe respiratory syndrome, with a mortality rate of 60%. Gross observations showed that infected lungs were highly edematous. Major histopathological changes in infected lungs included diffuse pneumonia and alveolar damage, with neutrophil-dominant inflammatory cellular infiltration, interstitial and alveolar edema, hemorrhage, and severe bronchiolitis/peribronchiolitis. In addition, H9N2 viral infection resulted in severe progressive hypoxemia, lymphopenia, and a significant increase in neutrophils, tumor necrosis factor-α and interleukin-6 in BALF. The features described above satisfy the criteria for acute respiratory distress syndrome (ARDS). Our data show that H9N2 viral infection resulted in ARDS in mice, and this may facilitate studies of the pathogenesis of future potential H9N2 disease in humans.

Introduction

H9N2 avian influenza viruses have become highly prevalent in poultry in many Eurasian countries since the early 1990s [9, 11]. Although these viruses generally cause only mild to moderate disease, they have been associated with severe morbidity and mortality in poultry as a result of coinfection with other pathogens [1]. Since 1998, H9N2 viruses have been isolated from pigs and humans with influenza-like illness in Hong Kong and Mainland China [4–6, 13, 18, 19, 24, 26, 31]. These findings indicate that the H9N2 avian influenza virus can also cross species barriers and expand its host range from avians to mammalians.

To date, H9N2 virus has usually caused relatively mild clinical signs in humans [4, 19]. However, recent studies have shown that infection of swine with H9N2 viruses causes significant morbidity and mortality [31]. Most of the diseased pigs showed typical respiratory signs, including fever, nasal and ocular discharge, coughing and dyspnoea. In some cases, paralysis associated with fatal disease was also observed [5]. Pigs are believed to serve as intermediate hosts for adaptation of avian influenza viruses that infect humans, and it has been shown that some of the H9N2 influenza viruses currently circulating in China have molecular features that allow them to preferentially bind to human α-2,6-NeuAcGal receptors [15, 24]. The recurring presence of H9N2 infections in pigs and humans has raised concerns about the possibility that H9N2 viruses are capable of evolving into pandemic strains [9, 26, 28].

G. Deng and J. Bi contributed equally to this manuscript.

G. Deng · J. Bi · F. Kong · X. Li · Q. Xu · J. Dong · M. Zhang · L. Zhao · Z. Luan · N. Lv · J. Qiao (✉)
Department of Pathophysiology, College of Veterinary Medicine, China Agricultural University, 100193 Beijing, People's Republic of China
e-mail: qiaojian010@yahoo.cn

G. Deng
College of Life Science, Ningxia University, 750021 Ningxia, People's Republic of China

Previous studies revealed that H9N2 viruses were able to infect mice without adaptation, and this resulted in different levels of lethality and kinetics of replication [9, 12]. More recently, it was demonstrated that an H9N2 virus showed enhanced replication and efficient transmission by direct contact in a ferret model [28]. It is well known that influenza viruses mainly cause pulmonary infection in animals and humans, but little information is available regarding H9N2 viral infection in lungs in mammals. Therefore, it is urgent to evaluate the pathology of pulmonary infection caused by currently circulating H9N2 viruses in an appropriate animal model. Here, an H9N2 avian virus with high lethality for mice, isolated recently from northern China, was used to address this in a mouse model. The results suggest that H9N2 viral infection induces a typical acute respiratory distress syndrome (ARDS) in mice that resembles the common features of ARDS [2, 29]. Our data may facilitate studies of the pathogenesis of future potential avian H9N2 disease in humans.

Materials and methods

Virus

The H9N2 virus used in this study was isolated from chickens in Hebei province of northern China in 2008 and was identified by means of hemagglutination inhibition and neuraminidase inhibition tests. The isolate was designated as A/Chicken/Hebei/4/2008(H9N2) (Ck/HB/4/08). The complete genome sequences of the virus are available from GenBank under accession numbers FJ499463–FJ499470. Our previous studies showed that this isolate was a reassortant virus containing A/Chicken/Beijing/1/94-virus-like HA, NA, and NS genes, an A/quail/HongKong/G1/97-like M gene, and A/Chicken/Shanghai/F/1998-like RNP genes. We analyzed its pathogenicity in chickens and mice in detail and found that it replicated efficiently in chicken lungs but did not cause obvious clinical signs in specific-pathogen-free (SPF) chickens. However, the mice exhibited high mortality rates and severe lung injury when inoculated with Ck/HB/4/08 virus without prior adaptation (data not shown). The virus was propagated in the allantoic cavities of 10-day-old embryonated SPF chicken eggs at 37°C for 72 h and stored at −80°C for use in all of the experiments described herein. The 50% mouse infectious dose (MID_{50}), 50% mouse lethal dose (MLD_{50}) and 50% egg infectious dose (EID_{50}) of Ck/HB/4/08 were determined by serial titration of virus in 10-day-old embryonated SPF chicken eggs at 37°C. Titers were calculated by the method of Reed and Muench as described previously [23]. All manipulations were performed under BSL-3+ laboratory conditions. Animal experiments were conducted according to established guidelines and approved by the Animal Care Committee of China Agricultural University (Beijing, People's Republic of China).

Animals and experimental protocols

To assess the pathogenicity of H9N2 virus in mice, six- to eight-week-old female SPF BALB/c mice, purchased from Beijing Laboratory Animal Research Center (Beijing, People's Republic of China), were housed in microisolator cages ventilated under negative pressure with HEPA-filtered air. During the experiment, mice had access to food and water ad libitum. A pilot experiment indicated that a dose of 1×10^4 MID_{50} of Ck/HB/4/08 H9N2 virus was optimal, because the course of the disease was prolonged and the infected mice presented obvious signs of respiratory illness. Therefore, in the present study, the mice were lightly anesthetized with diethyl ether and then inoculated intranasally (100 μl) with 1×10^4 MID_{50} of Ck/HB/4/08 H9N2 virus diluted in sterile saline. Mock-infected control animals were inoculated intranasally (100 μl) with an equivalent dilution of noninfectious allantoic fluid.

Two types of experiments were carried out in this study. The first experiment was to investigate clinical signs, gross lesions and mortality rates of H9N2-infected mice over a 14-day time period. In this experiment, 40 mice were divided randomly into two groups of 20 mice each. The H9N2-infected group was inoculated with Ck/HB/4/08 virus, and the control group received the noninfectious allantoic fluid, as described above. The animals' general behavior and clinical signs, including food intake, body weight, inactivity, anal temperature (measured with an infrared thermometer) and mortality, were monitored daily in each group for 14 days.

In the second experiment, we studied the features of ARDS induced in mice by H9N2 viral infection. Mice were divided randomly into two groups with 100 mice in each group. Since some infected mice died between day 4 and day 6 postinfection (p.i.), larger groups (100 per group) of mice were used. Ten mice of each group were chosen randomly, weighed and euthanized on days 1, 3, 5, 6, 7, 8, and 14 p.i., and the following parameters were observed: Lung injury was assessed by testing lung water content and histopathology. Arterial blood gas, white blood cell counts, tumor necrosis factor (TNF)-α and interleukin (IL)-6 levels in bronchoalveolar lavage fluid (BALF), and viral titers in the lungs were measured at different times.

Lung histopathology and assessment of lung water content

Three mice per group were weighed and sacrificed on days 1, 3, 5, 6, 7, 8, and 14 p.i. The whole lungs were removed.

The left lobes of the lungs were fixed in buffered 10% formalin and embedded in paraffin for histopathological evaluation. Five-micrometer-thick sections were stained with hematoxylin-eosin for light microscopy. The upper parts of the right lung lobes were used to determine the lung wet weight:body weight ratio and lung wet:dry weight ratio. The remaining lobes of the right lung were stored at −80°C until needed for determining the lung virus titer.

To assess lung water content, the lung wet weight:body weight ratio and lung wet:dry weight ratio were determined by weighing the right lung before and after oven desiccation at 80°C, and this was used as an indicator of lung edema [32]. Lung wet:dry weight ratio = weight of the whole wet lung/weight of the whole dry lung; lung wet weight:body weight ratio (%) = weight of the whole wet lung/body weight × 100%.

Virus titration

Virus titration was performed as described previously [23]. Lungs, kidneys, brains, livers, spleens, and hearts were collected and homogenized in cold phosphate-buffered saline on days 1, 3, 5, 6, 7, 8, and 14 p.i. Clarified homogenates were titrated for viral infectivity in embryonated chicken eggs from initial dilutions of 1:2. Viral titers were expressed as mean $\log_{10}$ EID_{50} per milliliter ± standard deviation (1 MID_{50} is about 1×10^3 EID_{50}).

Arterial blood gas analysis and peripheral blood leukocyte counts

After blood sample collection, blood gas analysis was conducted as described by Fagan et al. [7]. Briefly, arterial blood samples (0.3 ml) were collected in a heparinized syringe by percutaneous left ventricular sampling of lightly anesthetized mice spontaneously breathing room air. Blood gas analysis was immediately conducted with an IL 1640 pH/blood gas/electrolytes analyzer (Instrumentation Laboratory, Lexington, MA).

Heparinized blood samples (50 μl) were used for leukocyte counts at various time points. Cell numbers for three individual mice were determined in triplicate by counting with a hemocytometer. For differential counts, two blood smears from each mouse were stained with Wright stain, and the number of lymphocytes was determined. At least 100 cells were counted for each slide at a magnification of ×1,000 [27].

Neutrophil counts and measurement of TNF-α and IL-6 in BALF

According to the protocol described by Majeski et al. [14] and Nick et al. [17], bronchoalveolar lavage was performed immediately following sacrifice of the animal by cervical dislocation on the days indicated. In brief, the lungs were lavaged twice in situ with the chest cavity opened by midline incision with a total volume of 1.0 ml of saline (4°C) inserted through an endotracheal tube. The rate of recovery of BALF was not less than 90% for all of the animals tested. After the amount of fluid recovered was recorded, an aliquot of BALF was diluted 1:1 with 0.01% crystal violet dye and 2.7% acetic acid for leukocyte staining and erythrocyte hemolysis. The number of leukocytes in BALF was counted with a hemacytometer under a microscope. The remaining BALF was centrifuged (300×g, 10 min). Neutrophil differential counts were determined by Wright staining of a spun sample, on the basis of morphological criteria, under a light microscope with evaluation of at least 200 cells per slide. All slides were counted twice by different observers blinded to the status of the animal. The supernatant for cytokine analysis was immediately frozen and stored at −70°C. The concentrations of TNF-α and IL-6 were determined in BALF and serum, using ELISA kits (Sigma, St. Louis, MO).

Statistics

All data are expressed as means ± SD. Statistical analysis was performed with the SPSS statistical software package for Windows, version 13.0 (SPSS Inc., Chicago, IL). Differences between groups were examined for statistical significance by two-tailed Student t test. A p-value less than 0.05 was considered statistically significant.

Results

Clinical signs and gross pathological observations

Overall, infected mice presented a relatively acute clinical process. Some mice showed inactivity, altered gait, ruffled fur, inappetence, and an average weight loss of 9.4% on day 2 p.i. By day 3 p.i., most mice presented severe signs of respiratory disease, including visual signs of labored respiration and respiratory distress, and exhibited more severe inappetence, emaciation, and 15.7% weight loss. Sixty percent of the mice (12 of 20) died between days 4 and 6 p.i. Gross observation showed the infected lungs to be highly edematous, with profuse areas of hemorrhage (Fig. 1a). Retention of gas in the stomach was occasionally found in infected mice. Surviving mice began to recover on day 7 p.i. No obvious gross lesions were observed in the hearts, livers, brains or kidneys in infected mice.

Histopathological lesions in lungs of H9N2-infected mice

The infected mice displayed a similar histopathological pattern with severe diffuse pneumonia, characterized by inflammatory cellular infiltration, interstitial and alveolar edema and hemorrhage, as shown in Fig. 1. Diffuse pneumonia with severe alveolar damage was found in the whole lung (Fig. 1b) on day 4. Figure 1b–h showed the kinetic observations of lung lesions of H9N2-virus-infected mice. On day 3 p.i., lung lesions were characterized by edema around the small blood vessels (Fig. 1c, d, solid arrows), thickening of the alveolar wall, and dropout of mucous epithelium adhering to the surface of bronchioles (Fig. 1c, d, open arrows). On days 4–5 p.i., as shown in Fig. 1e, f, severe edema and neutrophil-dominant inflammatory cellular infiltration could be seen around small blood vessels (solid arrows) as well as diffuse pneumonia with

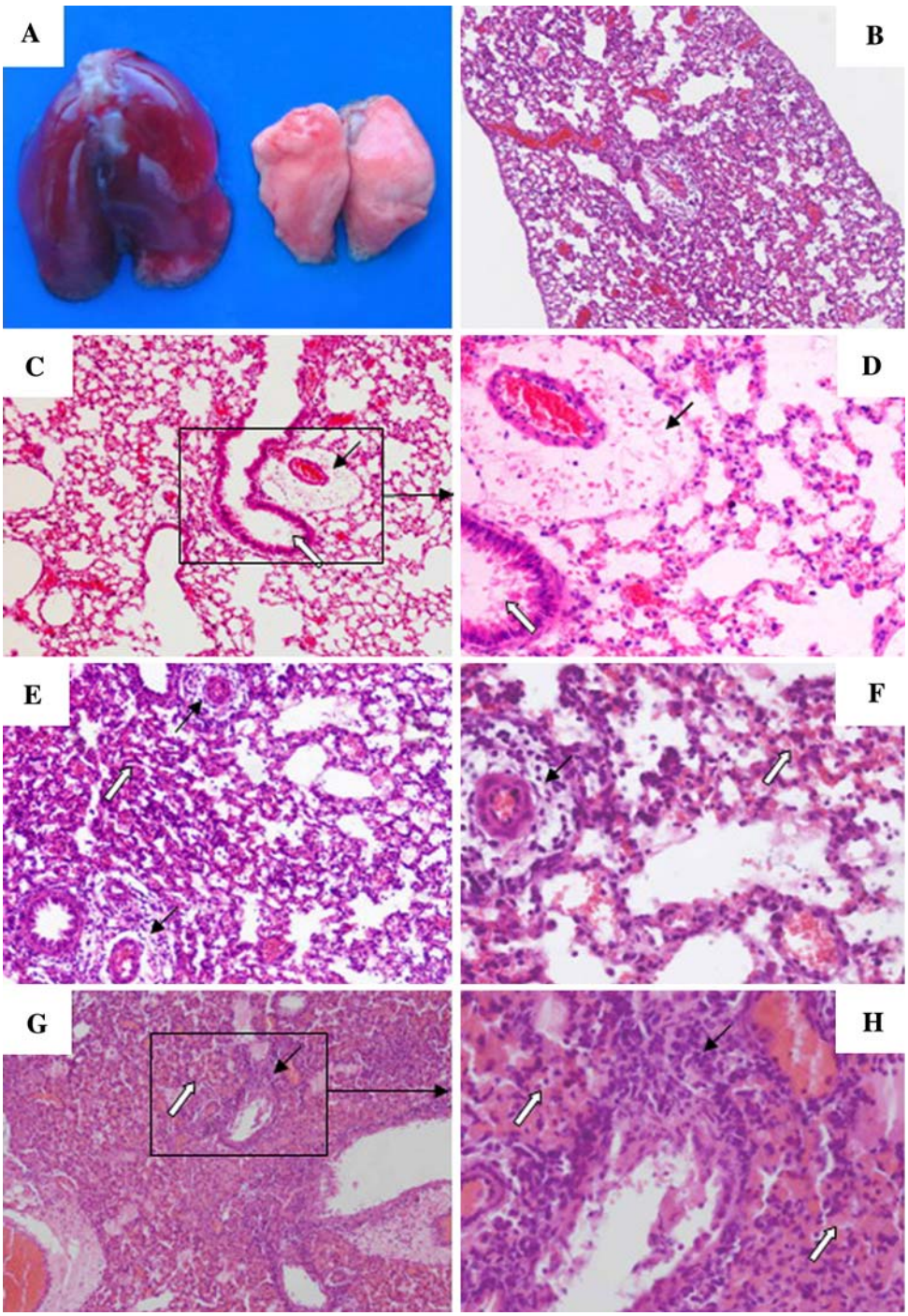

Fig. 1 Gross pathology and histopathology of H9N2-virus-infected lung. **a** shows severe edema, congestion and hemorrhage in the infected lung (*left*) on day 4 p.i. (*right*, control lung). Histopathology with hematoxylin-eosin staining in infected lung is shown in **b**–**h**. On day 3 p.i., thickening of the alveolar wall, interstitial edema around small blood vessels (**c**, **d**, *solid arrows*) and dropout of mucous epithelium adhering to the surface of bronchioles (**c**, **d**, *open arrows*) were observed. On days 4–5 p.i., diffuse pneumonia (**b**, **e**, **f**) with severe edema and neutrophil-dominant inflammatory cellular infiltration around small blood vessels (**e**, **f**, *solid arrows*) and severe alveolar injury (**e**, **f**, *open arrows*) were observed. By day 6 p.i., more severe diffuse pneumonia with alveolar lumens flooded with edema fluid mixed with fibrin, erythrocytes and inflammatory cells was observed (**g**, **h**, *open arrows*), as well as severe peribronchiolitis (**g**, **h**, *solid arrows*). Original magnification: **b**, **c**, **e**, **g** ×10; **d**, **f**, **h** ×40

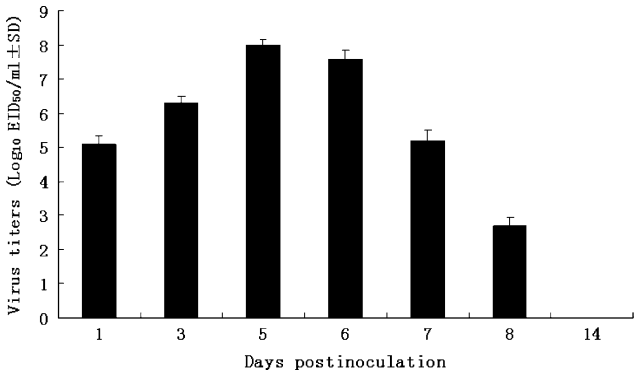

Fig. 2 Replication of H9N2 virus in mouse lungs. Mice were infected with 10^4 MID_{50} of Ck/HB/4/08 virus, tissues were collected on the indicated days p.i., and the virus was titrated in embryonated eggs. Mean viral titers based on three mice per group are expressed as $\log_{10}$ EID_{50} per milliliter ± SD. The limit of virus detection was $10^{1.2}$ EID_{50}/ml for lungs

inflammatory cellular infiltrate and erythrocytes in the alveolar lumens (open arrows). By day 6 p.i., the lesions in infected lungs became more severe. Alveolar lumens were flooded with edema fluid mixed with fibrin, erythrocytes, and inflammatory cells (open arrows in Fig. 1g, h). Severe peribronchiolitis (solid arrows in Fig. 1g, h), edema around blood vessels and severe hemorrhage were found (Fig. 1g, h). In addition, prominent dropout of bronchial epithelium and a great number of neutrophils, fibrin, and suppurative exudates infiltrating the bronchioles were also observed (solid arrows in Fig. 1g, h). In comparison, lungs from control mice had no apparent histological changes.

Replication of H9N2 virus in mouse tissues

Kinetic observation of H9N2 viral replication in mouse tissues indicated that the viruses in the lung replicated more efficiently than those in other tissues. Viral infection resulted in high titers of virus in the lungs on days 1–7 p.i. (Fig. 2). The peak viral titer was observed on day 5 p.i., reaching 8.0 $\log_{10}$ EID_{50}/ml. However, viral titers dropped to a relatively low level on day 8 p.i. Viruses were also isolated with lower titers from livers, kidneys, spleens, and hearts on days 3–6 p.i., but was not isolated from brains (data not shown).

Lung water content: edema

Fig. 3a shows the dramatic increased lung wet:dry weight ratios on days 3–8 p.i. ($p < 0.05$) after H9N2 viral infection. A similar change in lung wet weight:body weight ratios was also observed in infected lung, shown in Fig. 3b, with the peak value nearly fourfold that of the control on day 5 p.i.

Arterial blood gas analysis

Table 1 shows the time courses of arterial blood gas parameters in mice. The partial pressure of arterial oxygen (PaO_2), saturation of arterial oxygen (SaO_2), and pH value were slightly decreased, while partial pressure of arterial carbon dioxide ($PaCO_2$) was increased in infected mice on day 3 p.i. Subsequently, when most of the infected mice presented apparent clinical signs of respiratory distress at day 5 p.i., PaO_2 and SaO_2 also dramatically decreased as compared with the controls ($p < 0.01$).

Peripheral blood leukocyte counts

Figure 4a shows that the number of leukocytes in peripheral blood progressively decreased on days 1–6 p.i. in

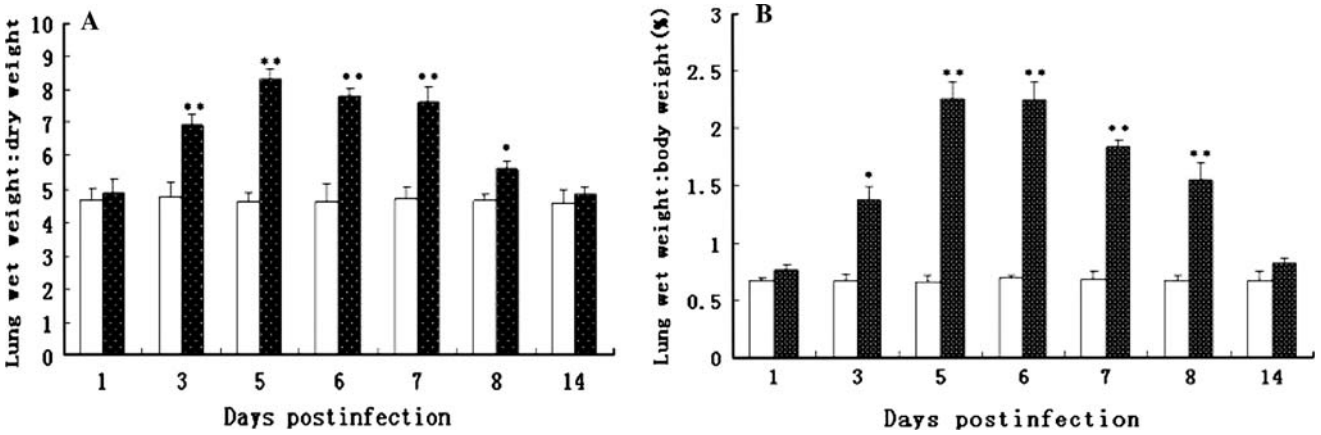

Fig. 3 Lung wet:dry weight ratios (**a**) and lung wet weight:body weight ratios (**b**) of H9N2-virus-infected mice. The means ± SD ($n = 4$) at each time point are shown. *Open bars* control group, *dotted bars* infection group. *$p < 0.05$ and **$p < 0.01$ compared with those in control mice

Table 1 Change in arterial blood gas in mice after H9N2 virus infection

Days postinfection	PaO_2 (kPa)		$PaCO_2$ (kPa)		pH value		SaO_2 (%)	
	Infection	Control	Infection	Control	Infection	Control	Infection	Control
3	10.98 ± 1.27	12.15 ± 1.12	5.52 ± 0.35	5.32 ± 0.47	7.33 ± 0.045	7.37 ± 0.042	86.5 ± 1.78†	92.1 ± 1.05
5	6.73 ± 1.02‡	12.35 ± 1.36	7.41 ± 0.57†	5.29 ± 0.38	7.11 ± 0.057	7.36 ± 0.039	77.9 ± 2.52‡	93.2 ± 0.88
6	7.06 ± 1.32‡	11.98 ± 1.47	7.15 ± 0.63†	5.26 ± 0.66	7.14 ± 0.081	7.35 ± 0.054	79.7 ± 3.12†	92.8 ± 1.13
8	9.34 ± 1.49	12.28 ± 1.08	6.63 ± 0.81	5.30 ± 0.75	7.21 ± 0.048	7.34 ± 0.053	83.4 ± 2.72†	92.7 ± 1.24
14	11.25 ± 1.76	12.19 ± 1.25	5.54 ± 0.74	5.27 ± 0.59	7.32 ± 0.055	7.36 ± 0.069	89.5 ± 2.46	91.8 ± 1.56

Values ($n = 4$) are expressed as means ± SD

† $p < 0.05$ and ‡ $p < 0.01$ compared with the control group

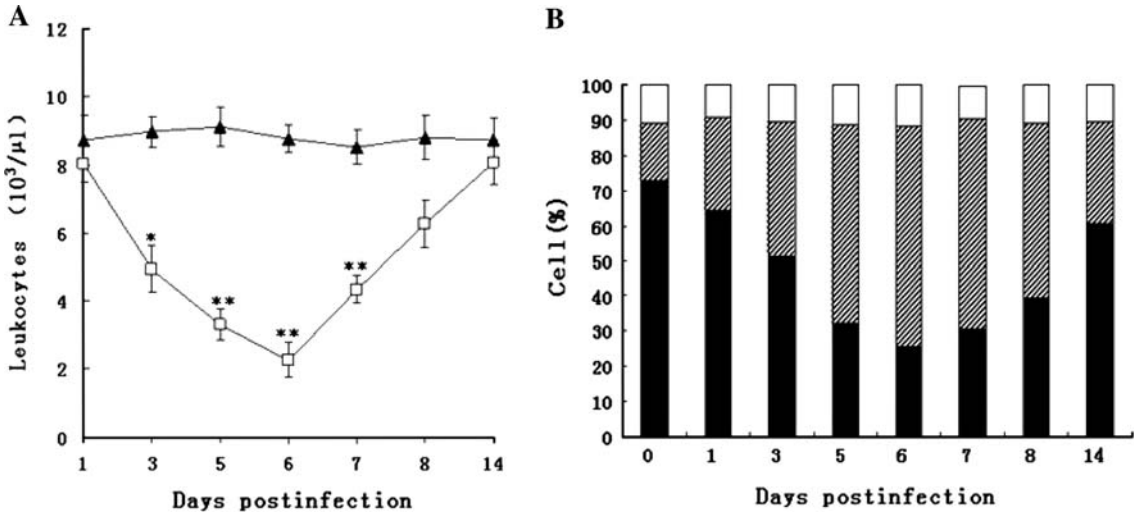

Fig. 4 Kinetic changes in circulating leukocytes (**a**) and blood differential counts (**b**) after H9N2 virus infection. The means ± SD ($n = 4$) at each time point are shown. **a** *Solid triangles* leukocytes of control mice, *open squares* leukocytes of infected mice, **b** *Open bars* monocytes, *striped bars* neutrophils, *solid bars* lymphocytes. *$p < 0.05$ and **$p < 0.01$ compared with those in control mice

infected mice compared with those in control mice. The lowest value was seen on day 6 p.i. Differential blood counts (Fig. 4b) revealed that the lymphocytes of infected mice dropped by about 50% on day 6 p.i. From day 7 p.i. onwards, both leukocytes and lymphocytes gradually increased in survived mice.

White blood cell summary and differential counts in BALF

Figure 5 shows the time course of white blood cell (WBC) summary and neutrophil counts in BALF on days 1, 3, 5, 6, 7, 8, and 14 p.i. The number of WBCs in infected mice increased gradually from day 3 p.i. and reached its peak, with about fourfold that of the control group, by day 6 p.i. Neutrophils in BALF increased dramatically from days 3–8 p.i., and the peak was approximately 14-fold greater than that of the control group on day 5 p.i.

Infection with H9N2 results in increased TNF-α and IL-6 levels in BALF and serum

Concentrations of TNF-α and IL-6 in BALF and serum were measured at different time points after H9N2 infection. As shown in Fig. 6a, levels of TNF-α in infected mice significantly increased on days 3–8 p.i. in BALF ($p < 0.05$) compared with those of the controls. TNF-α levels also rose significantly in serum on days 3–7 p.i. (Fig. 6b), but this alteration was not as significant as that in BALF. IL-6 levels increased slightly on days 5–8 p.i. in serum but increased dramatically in BALF on days 3–7 p.i. and reached a peak on day 6 p.i., with about 7.5 fold that of control mice.

Discussion

Previous studies have revealed that H9N2 viruses demonstrate different levels of lethality and kinetics of replication

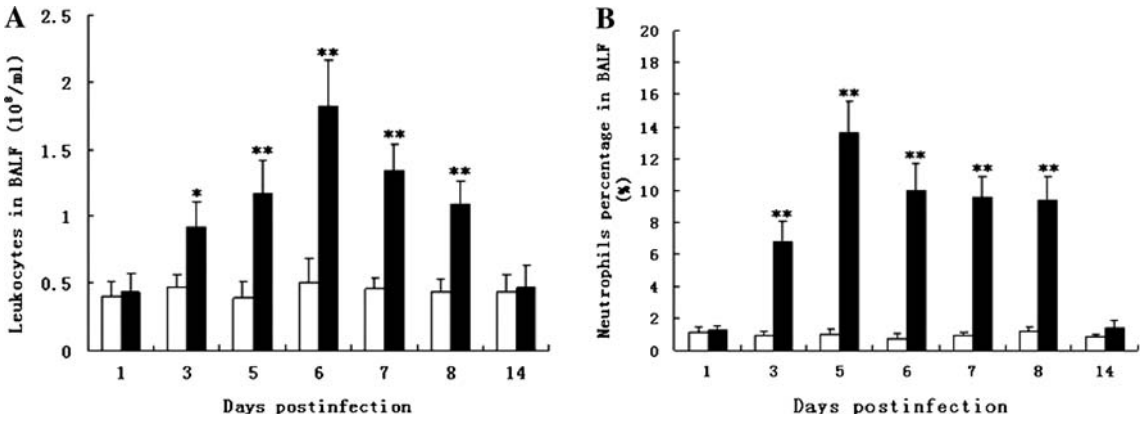

Fig. 5 Changes in leukocyte (**a**) and neutrophil counts (**b**) in BALF after H9N2 virus infection. The means ± SD ($n = 4$) at each time point are shown. *Open bars* control group, *solid bars* infection group. *$p < 0.05$ and **$p < 0.01$ compared with those in control mice

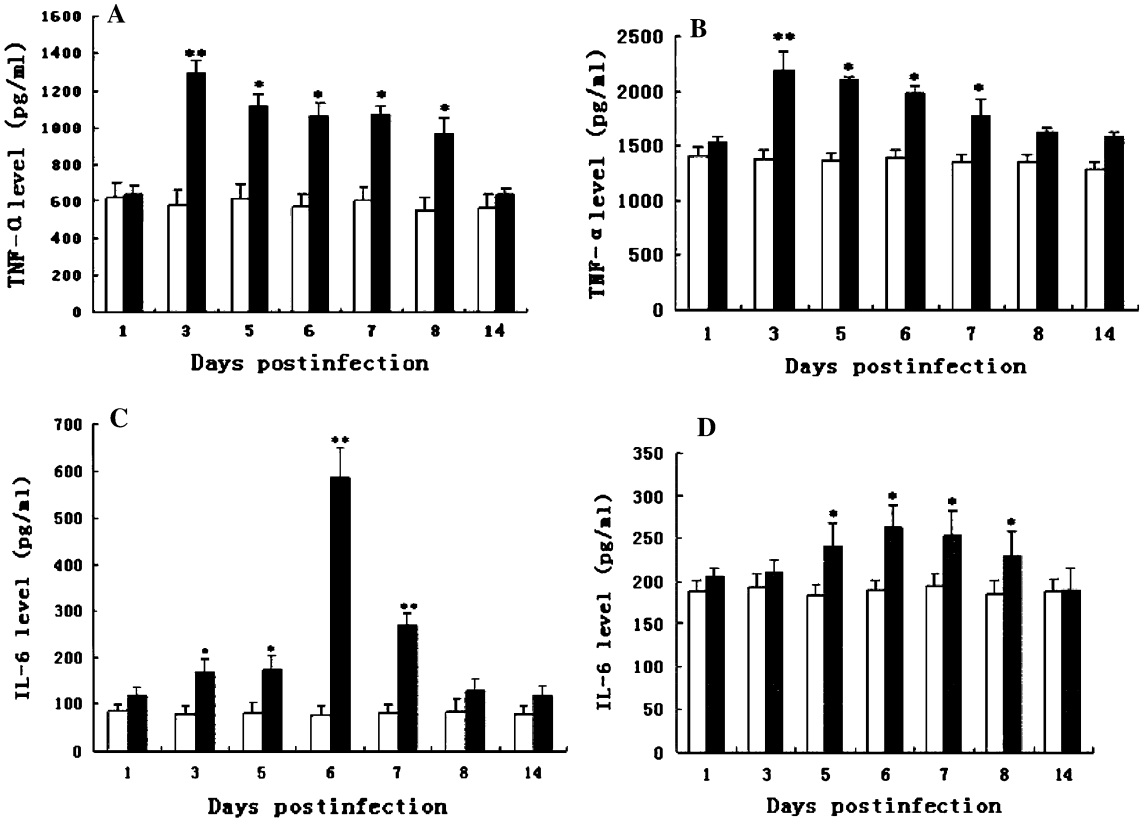

Fig. 6 TNF-α and IL-6 levels in BALF and serum of mice infected with H9N2 viruses. TNF-α in BALF (**a**) and in serum (**b**); IL-6 in BALF (**c**) and in serum (**d**). *Open bars* control group, *solid bars* infection group. *$p < 0.05$ and **$p < 0.01$ compared with those in control mice

in mice [9, 12, 30]. However, little information is available regarding H9N2 virus infection in lungs of mice. To address this, BALB/c mice were infected intranasally with 1×10^4 MID_{50} of Chicken/HB/4 H9N2 viruses, and the pathological changes in the lungs were evaluated. Our data show that H9N2 viral infection without prior adaptation caused severe respiratory disease with a high mortality of 60%. Most of the infected mice exhibited clinical signs of severe respiratory disease with obvious respiratory distress. Gross observation revealed highly edematous lungs in infected mice, which was also demonstrated by a dramatically increased lung wet:dry weight ratio and lung wet weight:body weight ratio. Histopathological evaluation showed that infected mice displayed a similar histopathological pattern, with severe diffuse pneumonia and alveolar damage, characterized by neutrophil-dominant

inflammatory cellular infiltration, interstitial and alveolar edema, hemorrhage, and severe bronchiolitis/peribronchiolitis. Additionally, arterial blood gas analysis demonstrated that the PaO_2 decreased dramatically and the $PaCO_2$ increased significantly when disease was exacerbated. This indicated that most of the infected mice developed progressive and severe hypoxemia consistent with the time course of clinical signs and pulmonary lesions for ARDS. The features described above satisfy the criteria of ARDS [2, 20–22, 29] and show that H9N2 viral infection resulted in the prominent ARDS in mice.

In comparison with ARDS in mice with H5N1 viral infection [32], H9N2 viral ARDS in mice shows a shorter course of disease. Most of the H9N2 virus-infected mice presented overt signs and died between days 4 and 6 p.i., while death of mice with H5N1 viral infection occurred between days 6 and 8 p.i. Besides this, the infected lungs are more edematous after H9N2 viral infection.

Observation of viral replication showed that the H9N2 viruses replicated efficiently in the lung. Viral infection resulted in high titers of viruses on days 1–7 p.i., with the peak viral titer on day 5 p.i. This was consistent with the time course of the severity of H9N2 viral respiratory disease in mice, indicating that high viral replication may be important for H9N2 viral disease pathogenesis. It is believed that TNF-α and IL-6 may play an important role in the development of ARDS [3, 10, 25]. In most studies, cytokines in patients with ARDS have been described as an inflammatory 'cascade' or 'network', and thus their actions were not easily manipulated [22]. H5N1 virus induced high levels of TNF-α and IL-6 in BALF and serum in the mouse ARDS model [32]. In this regard, our finding that H9N2 viral infection resulted in significantly increased TNF-α and IL-6 in BALF is similar to that of the previous study of H5N1 virus infection. The role of these cytokines in lung inflammation during H9N2 viral infection remains to be investigated.

A secondary intense neutrophil-predominant host inflammatory response is usually considered an important feature of ARDS. The inflammatory response triggered by direct or indirect insults to the lung involves the recruitment of blood leukocytes, the activation of tissue macrophages, and the production of a series of different mediators such as cytokines, chemokines and oxygen radicals [2, 3, 10, 16, 22, 25, 29]. Lung injury may be a direct consequence of this inflammatory response. In H9N2-virus-infected mice, we observed that circulating leukocytes dramatically decreased in the blood and that a great number of inflammatory cells infiltrated the lungs. In addition, the neutrophils in BALF increased approximately 14-fold compared to control mice on day 5 p.i. These results suggested that a great number of leukocytes, especially neutrophils, were recruited from the bloodstream and sequestrated mainly in the lungs, and this might be involved in the host inflammation response and severe pulmonary lesions induced by H9N2 viral infection.

Some studies have shown that H9N2 viruses could cause upper respiratory tract illnesses in humans [19]. Subsequent studies have revealed that H9N2 viruses can also infect pigs and cause typical respiratory signs with significant morbidity and mortality [6, 31]. Further investigation demonstrated that currently circulating H9N2 influenza viruses in China continued to evolve and generate multiple genotypes [8, 13, 18], raising the possibility that the H9N2 virus might increase pathogenicity and transmissibility in humans and would be a potential threat to the human population. Our findings highlight the serious potential threat of H9N2 for human health.

In summary, our data show that H9N2 viral infection induced typical ARDS in mice, which might facilitate studies of the pathogenesis of future potential avian H9N2 disease in humans.

Acknowledgments This work was supported by the National Natural Science Foundation of China (Grant number: 30972163 and 30571398) and by the Program for Cheung Kong Scholars and Innovative Research Team in University of China (No. IRT0866).

References

1. Bano S, Naeem K, Malik SA (2003) Evaluation of pathogenic potential of avian influenza virus serotype H9N2 in chickens. Avian Dis 47:817–822
2. Bernard GR (2005) Acute respiratory distress syndrome: A historical perspective. Am J Respir Crit Care Med 172:798–806
3. Bhatia M, Moochhala S (2004) Role of inflammatory mediators in the pathophysiology of acute respiratory distress syndrome. J Pathol 202:145–156
4. Butt KM, Smith GJD, Chen H, Zhang LJ, Leung YHC, Xu KM, Lim W, Webster RG, Yuen KY, Peiris JSM, Guan Y (2005) Human infection with an avian H9N2 influenza A virus in Hong Kong in 2003. J Clin Microbiol 43:5760–5767
5. Cong YL, Pu J, Liu QF, Wang S, Zhang GZ, Zhang XL, Fan WX, Brown EG, Liu JH (2007) Antigenic and genetic characterization of H9N2 swine influenza viruses in China. J Gen Virol 88:2035–2041
6. Cong YL, Wang CF, Yan CM, Peng JH, Jiang ZL, Liu JH (2008) Swine infection with H9N2 influenza viruses in China in 2004. Virus Genes 36:461–469
7. Fagan KA, Fouty BW, Tyler RC, Morris KG Jr, Hepler LK, Sato K, LeCras TD, Abman SH, Weinberger HD, Huang PL, McMurtry IF, Rodman DM (1999) The pulmonary circulation of homozygous or heterozygous eNOS-null mice is hyperresponsive to mild hypoxia. J Clin Invest 103:291–299
8. Guan Y, Shortridge KF, Krauss S, Webster RG (1999) Molecular characterization of H9N2 influenza viruses: were they the donors of the "internal" genes of H5N1 viruses in Hong Kong? Proc Natl Acad Sci USA 96:9363–9367
9. Guo YJ, Krauss S, Senne DA, Mo IP, Lo KS, Xiong XP, Norwood M, Shortridge KF, Webster RG, Guan Y (2000) Characterization of the pathogenicity of members of the newly

established H9N2 influenza virus lineages in Asia. Virology 267:279–288
10. Headley AS, Tolley E, Meduri GU (1997) Infections and the inflammatory response in acute respiratory distress syndrome. Chest 111:1306–1321
11. Lee CW, Song CS, Lee YJ, Mo IP, Garcia M, Suarez DL, Kim SJ (2000) Sequence analysis of the hemagglutinin gene of H9N2 Korean avian influenza viruses and assessment of the pathogenic potential of isolate MS96. Avian Dis 44:527–535
12. Li CJ, Yu KZ, Tian GB, Yu DD, Liu LL, Jing B, Ping JH, Chen HL (2005) Evolution of H9N2 influenza viruses from domestic poultry in Mainland China. Virology 340:70–83
13. Lin YP, Shaw M, Gregory V, Cameron K, Lim W, Klimov A, Subbarao K, Guan Y, Krauss S, Shortridge K, Webster R, Cox N, Hay A (2000) Avian-to-human transmission of H9N2 subtype influenza A viruses: relationship between H9N2 and H5N1 human isolates. Proc Natl Acad Sci USA 97:9654–9658
14. Majeski EI, Paintlia MK, Lopez AD, Harley RA, London SD, London L (2003) Respiratory reovirus 1/L induction of intraluminal fibrosis, a model of bronchiolitis obliterans organizing pneumonia, is dependent on T lymphocytes. Am J Pathol 163:1467–1479
15. Matrosovich MN, Krauss S, Webster RG (2001) H9N2 influenza A viruses from poultry in Asia have human virus-like receptor specificity. Virology 281:156–162
16. Ng WF, To KF, Lam WL, Ng TK, Lee KC (2006) The comparative pathology of severe acute respiratory syndrome and avian influenza A subtype H5N1—a review. Hum Pathol 37:381–390
17. Nick JA, Young SK, Brown KK, Avdi NJ, Arndt PG, Suratt BT, Janes MS, Henson PM, Worthen GS (2000) Role of p38 mitogen-activated protein kinase in a murine model of pulmonary inflammation. J Immunol 164:2151–2159
18. Peiris JSM, Guan Y, Markwell D, Ghose P, Webster RG, Shortridge KF (2001) Cocirculation of avian H9N2 and contemporary "human" H3N2 influenza A viruses in pigs in southeastern China: potential for genetic reassortment? J Virol 75:9679–9686
19. Peiris M, Yuen KY, Leung CW, Chan KH, Ip PL, Lai RW, Orr WK, Shortridge KF (1999) Human infection with influenza H9N2. Lancet 354:916–917
20. Pelosi P, Brazzi L, Gattinoni L (2002) Prone position in acute respiratory distress syndrome. Eur Respir J 20:1017–1028
21. Pelosi P, D'Onofrio D, Chiumello D, Paolo S, Chiara G, Capelozzi VL, Barbas CSV, Chiaranda M, Gattinoni L (2003) Pulmonary and extrapulmonary acute respiratory distress syndrome are different. Eur Respir J 22:48–56
22. Puneet P, Moochhala S, Bhatia M (2005) Chemokines in acute respiratory distress syndrome. Am J Physiol Lung Cell Mol Physiol 288:L3–L15
23. Reed LJ, Muench HA (1938) A simple method of estimating fifty percent endpoints. Am J Epidemiol 27:493–497
24. Saito T, Lim W, Suzuki T, Suzuki Y, Kida H, Nishimura SI, Tashiro M (2001) Characterization of a human H9N2 influenza virus isolated in Hong Kong. Vaccine 20:125–133
25. Schutte H, Lohmeyer J, Rosseau S, Ziegler S, Siebert C, Kielisch H, Pralle H, Grimminger F, Morr H, Seeger W (1996) Bronchoalveolar and systemic cytokine profiles in patients with ARDS, severe pneumonia and cardiogenic pulmonary oedema. Eur Respir J 9:1858–1867
26. Shi WF, Gibbs MJ, Zhang YZ, Zhang Z, Zhao XM, Jin X, Zhu CD, Yang MF, Yang NN, Cui YJ, Ji L (2008) Genetic analysis of four porcine avian influenza viruses isolated from Shandong, China. Arch Virol 153:211–217
27. Tumpey TM, Lu X, Morken T, Zaki SR, Katz JM (2000) Depletion of lymphocytes and diminished cytokine production in mice infected with a highly virulent influenza A (H5N1) virus isolated from humans. J Virol 74:6105–6116
28. Wan H, Sorrell EM, Song H, Hossain MJ, Ramirez-Nieto G, Monne I, Stevens J, Cattoli G, Capua I, Chen LM, Donis RO, Busch J, Paulson JC, Brockwell C, Webby R, Blanco J, Al-Natour MQ, Perez DR (2008) Replication and transmission of H9N2 influenza viruses in ferrets: evaluation of pandemic potential. PLoS ONE 3:e2923
29. Wheeler AP, Bernard GR (2007) Acute lung injury and the acute respiratory distress syndrome: a clinical review. Lancet 369:1553–1564
30. Wu R, Sui ZW, Zhang HB, Chen QJ, Liang WW, Yang KL, Xiong ZL, Liu ZW, Chen Z, Xu DP (2008) Characterization of a pathogenic H9N2 influenza A virus isolated from central China in 2007. Arch Virol 153:1549–1555
31. Xu C, Fan W, Wei R, Zhao H (2004) Isolation and identification of swine influenza recombinant A/Swine/Shandong/1/2003(H9N2) virus. Microbes Infect 6:919–925
32. Xu T, Qiao J, Zhao L, Wang G, He G, Li K, Tian Y, Gao M, Wang J, Wang H, Dong C (2006) Acute respiratory distress syndrome induced by avian influenza A (H5N1) virus in mice. Am J Respir Crit Care Med 174:1011–1017